Probabilistic Seismic hazard assessment and focal mechanism mapping of Minab fault zone and the Strait of Hormoz

Tavakolizade, N.[1], Sadidkhouy, A.[2]

[1]M.Sc. student, Institute of Geophysics, University of Tehran, Tehran, Iran
[2] Assistant Professor, Institute of Geophysics, University of Tehran, Tehran, Iran
E-mail: (nasrintavakoli@ut.ac.ir)

1. ABSTRACT

This study focuses on probabilistic hazard assessment of Minab transition zone, its accompanied fault zones, and the strait of Hormoz. On the one hand, different tectonic regimes and different convergence angle (confirmed by GPS based velocity measurements), influence Minab fault zone and the strait of Hormoz. On the other hand, this location includes a large population and is one of the main Iranian trading harbors. Seismicity of this region are studied by mapping faults and gathering a precise and complete earthquake data set of historical (based on Ambraseys and Melville (1982) Iran historical earthquake records) and instrumental data based on IRIS, IRSC, ISC, and USGS data sets. Investigated catalogue consist of 8715 earthquakes. Fault map of this area showed plenty of major and thrust faults. The seismotectonic map accompanied by CMT focal mechanisms plotted to demonstrating earthquake mechanisms. Strike-slip, reverse, over-thrusting, and oblique movements are dominating fault mechanisms in the study area. Probabilistic hazard assessment is done based on four sources, elected by fault trends, focal mechanisms, and earthquake accumulation schemes in order to assess seismic hazard potentials. Activity rate (N), b-value, and magnitude of completeness evaluated utilizing Zmap software and Gutenberg-Richter relation. KIJKO implemented to calculating earthquake engineering parameters (lambda and Beta). CRISIS software used for plotting SA (Spectral Acceleration) maps for two recurrence time (RT; 50, 475 years) and two different periods (0.2, 0.8). Maximum evaluated SA for 50 and 475 recurrence time are 0.98(g), 1.65(g) (of 0.2 Time period); and 0.38(g), 0.57(g) (of 0.8 Time period), respectively. Uniform hazard response spectrum (UHRS) for 2, 5, 10, and 64 percent of probability of exceedance plotted. Obtained results are in good agreement with tectonic regimes of the study area and taking them into account while constructing infrastructures and buildings improves location specification.

2. **KEYWORDS:** Crisis; Minab; PGA; Seismic hazard assessment; Tectonic regimes; The strait of Hormoz.

3. INTRODUCTION

Study area (fig 1) is located in longitude and latitude between 29°N to 25°38´N, and 55°30´E to 58°30´E, respectively. Strait of Hormoz and Minab fault system constitute a transition boundary between the Zagros fold and trust belt and Makran accretionary prism (Pyret et al., 2009; Regard et al., 2004). Two main fault systems are responsible for accommodating deformation in this transition zone. Minab-Zendan and Sabzevaran-Jiroft fault system. Through Makran subduction zone, the oceanic part of Arabian plate is subducting beneath Eurasian plate since Cretaceous (Mirzaei et al., 1998). Minab and Sabzevaran fault system accommodate 5.1±1.3 or 1.3±6.6 and 6.2±0.7 mm yr^{-1} of strike-slip rates (Regard et al., 2004) which is a proportion of oblique convergence of the Arabian-

Eurasian plates. On the other hand, the present-day convergence rate obtained by Vernant et al., in (2004) showed about 9±2mm yr-1 in southeastern Zagros fold and trust belt which is in good agreement with GPS measurement by Hessami et al., (2006) that gained 9±3mm yr-1 for the same location. The Makran accretionary prism undergone reverse faulting with convergence 19±2mm yr-1 rate (Vernant et al., in 2004). Zagros simply folded and thrusted belt (ZFTB) accommodate a major proportion of reverse faulting of the Arabian convergence and on the contrary to this fact, this part of ZFTB rarely shows syn-rupture faulting (Walker et al., 2005). Therefore, studying seismic hazard assessment in this area is crucial due to the complications.

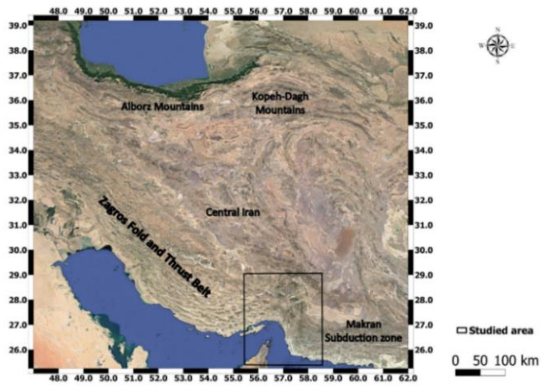

Fig1: Mountain belt in Iran. The inset shows the studied area at the critical connection of two active tectonic zone.

4. Seismicity and faults

The implemented data set include historical and instrumental data and the moment magnitude were used. These data set (contained IRIS, IRSC, ISC, and USGS) gathered and solidified and completed by using Mousavi et al., (2014) paper introduced relation. Historical data gathered based on Ambraseys and Melville (1982) which are the earthquakes happened before the 20th century and there are uncertainties along with time and location of them (fig 2).

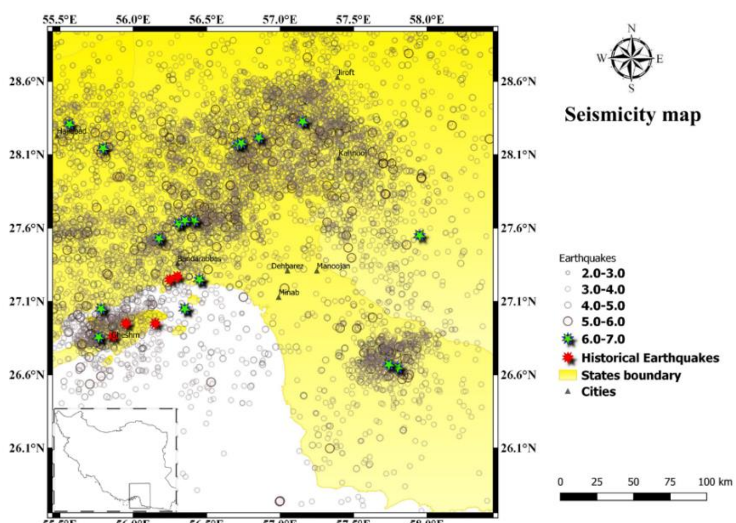

Fig 2: Seismicity map of the study area (the inset shows the location of the plotted map).

The collected data base contains 1352 number of 20th century earthquakes with 12 magnitudes more than 6 (M_w) (fig 2). The whole catalogue contained 8715 earthquakes (fig 2). Western boundary of Makran subduction zone is occupied by Minab fault zone which connects the region to the convergence zone of ZFTB (fig 3). Sharp divergence in the basement of Minab fault zone are evident in seismic reflection cross sections and seismicity differs in both sides of the zone from intense seismic activity in Zagros to relative quiescence through western Makran (Mirzaei et al., 1998). These results in complex tectonic activity and earthquake energy release in the study area. Two different faults are widely investigated in Zagros nodal planes, 0°-30° and 30°-60°. The latter group mostly shows reverse mechanism (Talebian and Jackson, 2004).

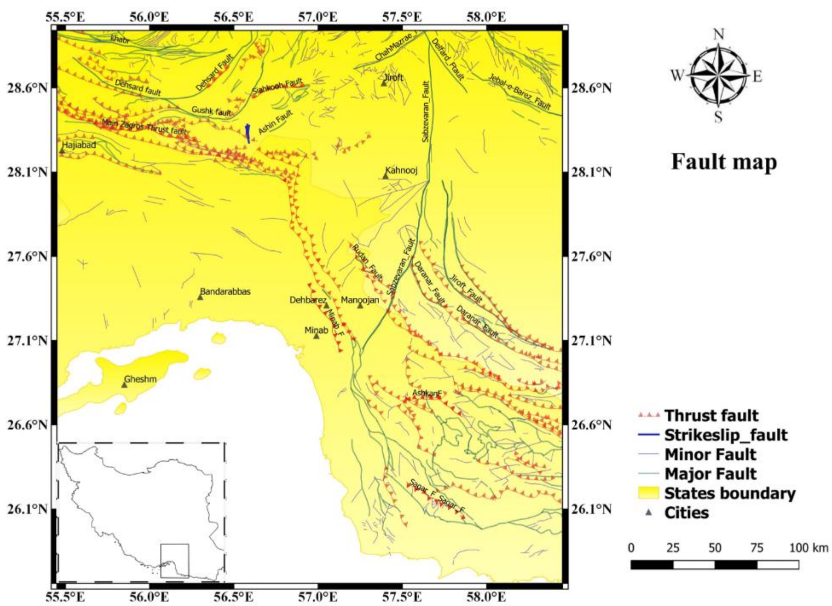

Fig 3: Fault map in Minab fault zone and the strait of Hormoz (the inset shows the location of the study area).

Plenty of active faults are located in the studied area; Minab faulted zone demonstrated strike-slip (until the initiation of Quaternary era) and over thrusting as its present-day movement. Main Zagros thrust fault (reverse mechanism), Sabzevaran and Jiroft fault system with right-lateral movement (Hessami and Jamali, 2006), Dehsard reverse fault, Gushk and Pashgiram reverse fault, Ashin fault with strike-slip left-lateral mechanism, Roudan fault with reverse mechanism (Berberian, 1976), Chahmazraeh fault showing left-lateral strike-slip movements and Jebal Barez fault showing simultaneous reverse strike-slip and thrust movements (Boshrabadi., et al, 2018) (fig3). Seismotectonic map of the Minab and the strait of Hormoz have been plotted based on faults of 1:250000 scale geological maps, earthquake data base and CMT focal mechanisms (fig4).

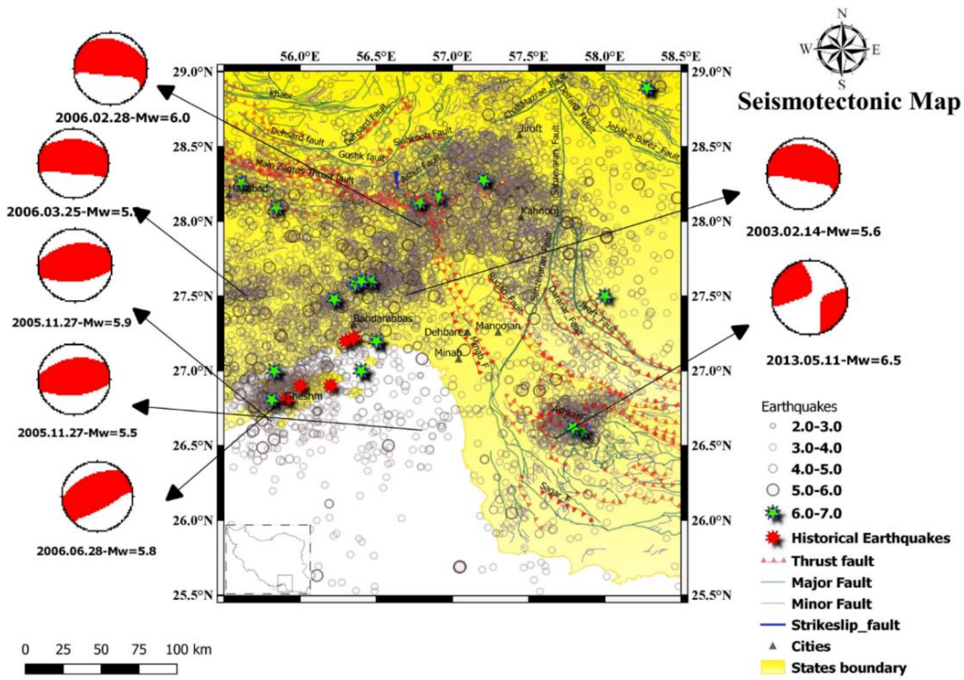

Fig4: Seismotectonic map of the studied area (the inset shows the location of the studied area).

5. Probabilistic seismic hazard assessment

In order to probabilistically analyze seismic hazard in a tectonically active zone, distinguishing seismic sources is crucial. Faulting mechanism (the type of sources), seismicity, seismotectonic zonation, earthquakes arrangement, and tectonic regime influence source characterization process. According to this facts, four sources have been chosen to basis the hazard analysis (fig5). Activity rate (N), b-value, and magnitude of completeness are calculated in each source based on Gutenberg-Richter method and acquired data base by implementing Zmap plugin in MATLAB software.

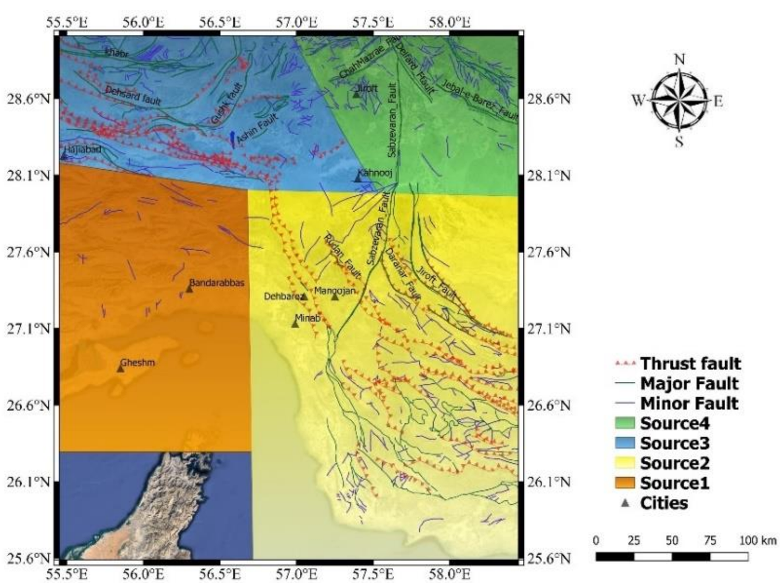

Fig 5: Seismic sources defined based on tectonic and seismic activity assessments in the studied area.

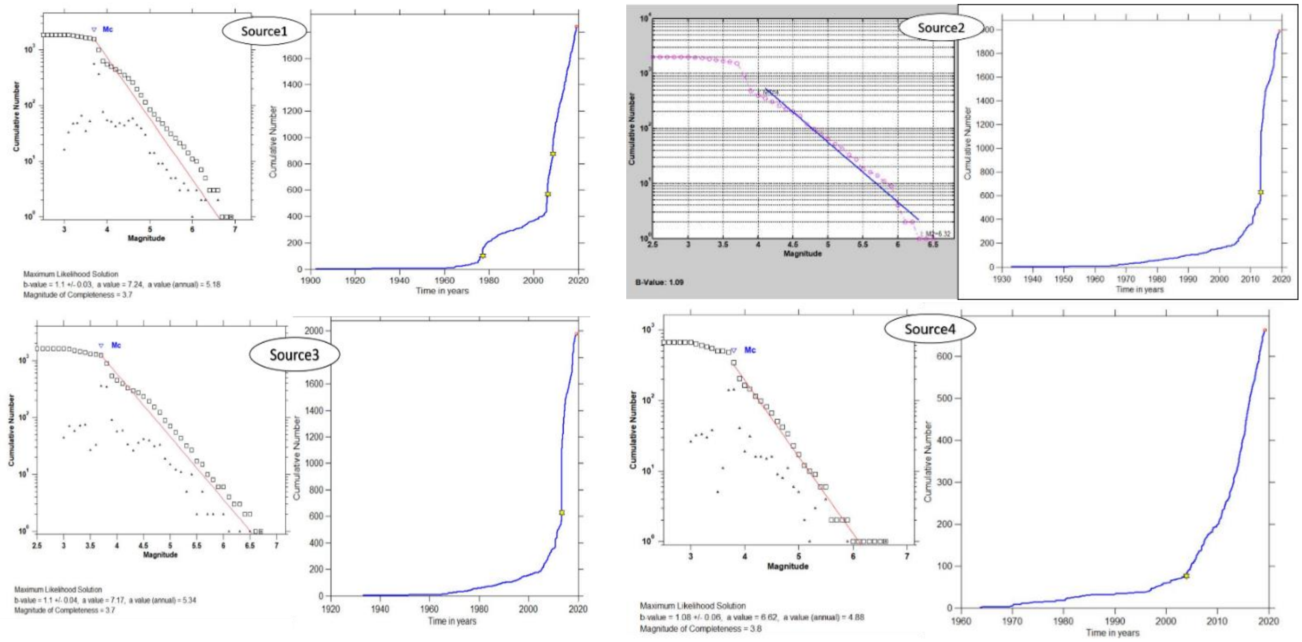

Fig 5: Cumulative variation of earthquakes in different decades of data acquisition and by increasing the magnitude. The characterized Mc and b-value source plotted in each source.

For this step, earthquake clusters must be eliminated based on their spatial and chronological distribution. Dependent events are characterized by their long offsets and short duration (Christophersen et al., 2011). The implemented method here is Rasenberg's (1985), which is based on spatial and time differences between events and alternated network-based methods.

(a)

```
      Maximum OBSERVED magnitude Xmax =  6.90
SECOND Maximum OBSERVED magnitude Xmax =  6.60

M_max is determined according to Kijko-Sellevoll (Cramers Approximation)

PRIOR b-value & SD[of PRIOR b] = 1.10      .030

                    RESULTS
                   =========
Beta   =  2.51 +-   .03  (b =  1.09 +-   .01)
Lambda =     6.16 +-     .19  (for Mmin =  3.60)
M_max  =  6.90 +-   .20  (for SIG(Xmax) =   .20)

Transmission coefficient =  1.67
```

(b)

```
      Maximum OBSERVED magnitude Xmax =  6.70
SECOND Maximum OBSERVED magnitude Xmax =  6.50

M_max is determined according to Kijko-Sellevoll (Cramers Approximation)

PRIOR b-value & SD[of PRIOR b] = 1.10      .040

                    RESULTS
                   =========
Beta   =  2.29 +-   .04  (b =   .99 +-   .02)
Lambda =   10.17 +-     .39  (for Mmin =  3.60)
M_max  =  6.70 +-   .20  (for SIG(Xmax) =   .20)

Transmission coefficient =  2.05
```

(c)

```
      Maximum OBSERVED magnitude Xmax =  6.50
SECOND Maximum OBSERVED magnitude Xmax =  6.20

M_max is determined according to Kijko-Sellevoll (Cramers Approximation)

PRIOR b-value & SD[of PRIOR b] = 1.09      .130

                    RESULTS
                   =========
Beta   =  1.72 +-   .08  (b =   .75 +-   .04)
Lambda =     3.94 +-     .22  (for Mmin =  3.90)
M_max  =  6.50 +-   .20  (for SIG(Xmax) =   .20)

Transmission coefficient =  1.21
```

(d)

```
      Maximum OBSERVED magnitude Xmax =  6.60
SECOND Maximum OBSERVED magnitude Xmax =  5.90

M_max is determined according to Kijko-Sellevoll (Cramers Approximation)

PRIOR b-value & SD[of PRIOR b] = 1.08      .060

                    RESULTS
                   =========
Beta   =  2.77 +-   .09  (b =  1.20 +-   .04)
Lambda =     3.43 +-     .25  (for Mmin =  3.70)
M_max  =  6.60 +-   .20  (for SIG(Xmax) =   .20)

Transmission coefficient =  6.69
```

Fig 6: Engineering seismology parameters retrieved from KIJKO, a) Source 1, b) Source 2, c) Source 3, d) Source4

The plots of umulative abundance of earthquakes (fig 5) in each source, shows a sudden rise due to the emergence of Iranian seismological center stations which is obvious in all four chosen sources. Defining a reliable magnitude of completeness (Mc) is necessary while investigating seismic hazard potentials and seismicity in an area (Woessner and Wiemer, 2005). In this study, Mc and b-value in each source after delustering the catalogue (fig 5).

By utilizing KIJKO software, earthquake engineering parameters, return period, density and probability distribution retrieved based on the declustered data base. The minimum and maximum magnitude of the catalogue of introduced, and the maximum number of 999 earthquake included in each part for every source. Four number of outputs obtained for four selected sources by KIJKO. Since the included magnitudes in this study are the range of earthquakes with destruction potential, the magnitudes less than Mc in each source are excluded (fig 6).

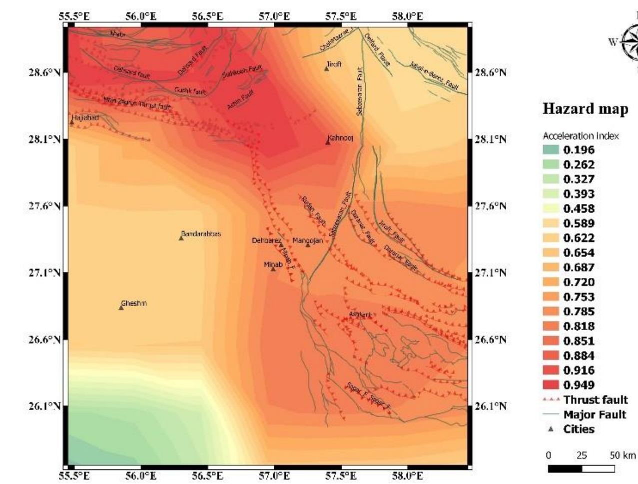

a) Period 0.2 and RT=50yr

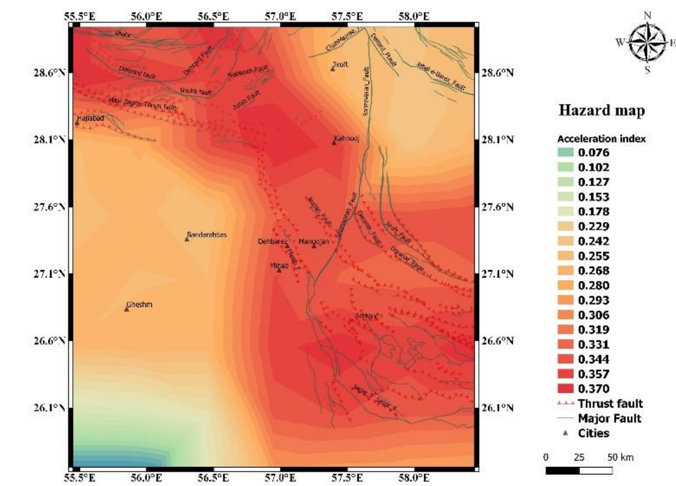

b) Period 0.8 and RT=50yr

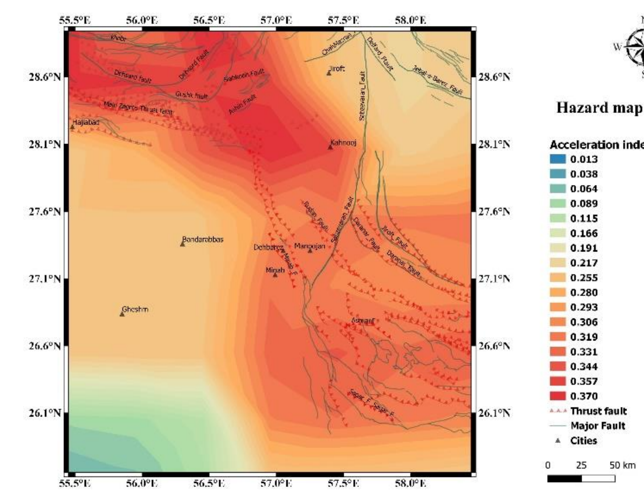

c) Period 0.2 and RT=475yr

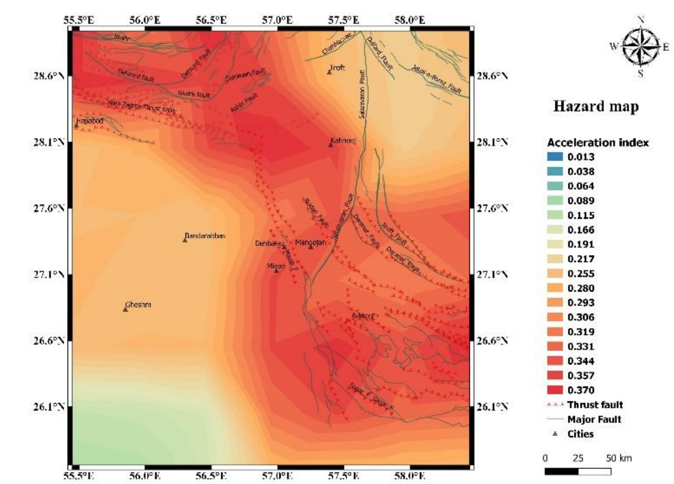

d) Period 0.8 and RT=475yr

Fig7: Seismic hazard map (SA-(g)) of the strait of Hormoz and Minab transition tectonic zone.

Effect of different attenuation mechanisms result in reduction of earthquakes strong ground motion. There exists different attenuation relation which parametrize this mechanism to taking into account while investigating seismic hazard conditions based on magnitude and focal distance. This research neglected the site effect and implemented Campbell and Bozorgnia, (2008) attenuation relation. Seismic hazard assessment accomplished based on Crisis software, KIJKO outputs, and the attenuation relation for different recurrence time (RT) (fig 7).

6. Discussion and conclusion

Minab tectonic transition zone and strait of Hormoz seismic hazard assessment show complex tectonic activity and focal mechanisms (fig 4) in seismotectonic maps, caused by different tectonic regimes on two sides of this faulted and active zone. For infrastructure construction plans due to the dense population and an important trade harbor of Iran, SA maps would be beneficial. The obtained hazard maps (fig 7) showed that the hazardous area in this study is located on high Zagros, Makran accretionary prism, and of course the transition zone of Minab and Sabzevaran fault zone. Zagros simply folded belt (since it accommodates detachment zone consist of Hormoz salt (Koyi and Hessami, 2000)) and Central Iranian block at the southwest and northeast of the study area, respectively; showed the lowest acceleration and risk. These maps showed that for the goal of building a persistent two floor building (period=0.2), for a hazard with 50-year recurrence time, the NW and SE of the study area have the highest risk potential. The same situation exists on the map of 475 year (RT) and period equal to 0.8. For the period of 0.8 and 50 and 475 year of recurrence time, SA(g) variations and hazard potentials plotted (fig 7). Uniform hazard spectra (UHS) plotted for 2, 5, 10, 64 percent probabilities of exceedance (fig 8). These spectra should be considered for scaling design spectrum for a specified probability of exceedance while constructing multistory buildings.

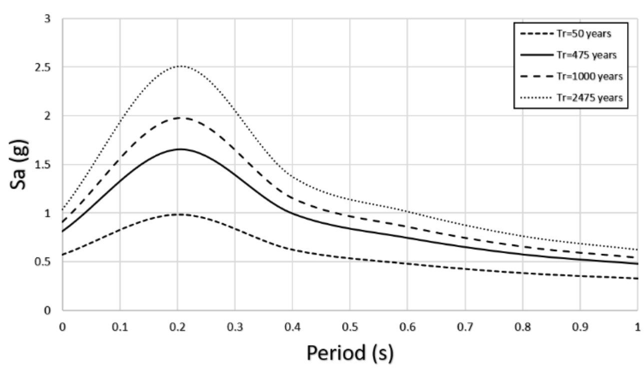

Fig 8: Uniform Hazard Response Spectra (UHS) for five different recurrence time (2, 5, 10, 64 percent probabilities of exceedance).

1. References

- Ambraseys, N.N. and Melville, C.P. (1982) A History of Persian Earthquakes. Cambridge University Press, Cambridge, England, 219p.

- Berberian, M. (1976). Pre-quaternary faults in Iran. Geological Survey of Iran, 39, 259-269.

-Boshrabadi, A. R., Khatib, M. M., Raeesi, M., Mousavi, S. M., & Djamour, Y. (2018). Geometric-kinematic characteristics of the main faults in the W-SW of the Lut Block (SE Iran). Journal of African Earth Sciences, 139, 440-462.

- Campbell KW, Bozorgnia Y. (2008). NGA ground motion model for the geometric mean horizontal component of PGA, PGV, PGD and 5% damped linear elastic response spectra for periods ranging from 0.01 to 10 s. Earthquake Spectra. 24(1):139-71.

- Christophersen, A., Gerstenberger, M. C., Rhoades, D. A., Stirling, M. W., (2011). Quantifying the effect of declustering on probabilistic seismic hazard. In Proc. of the Ninth Pacific Conf. on Earthquake Engineering: Building an Earthquake-Resilient Society.

- Hessami, K., & Jamali, F. (2006). Explanatory notes to the map of major active faults of Iran. Journal of Seismology and Earthquake Engineering, 8(1), 1-11.

- Koyi HA, Hessami K, Teixell A. (2000). Epicenter distribution and magnitude of earthquakes in fold-thrust belts: Insights from sandbox models. Geophysical Research Letters. 27(2):273-6.

- Kramer, S. L., (1996). Geotechnical earthquake engineering. Pearson Education India.

- Mirzaei N, Mengtan G, Yuntai C. (1998) Seismic source regionalization for seismic zoning of Iran: major seismotectonic provinces. Journal of earthquake prediction research.7:465-95.

- Mousavi-Bafrouei SH, Mirzaei N, Shabani E. (2015). A declustered earthquake catalog for the Iranian Plateau. Annals of Geophysics. 57(6).

- Peyret M, Djamour Y, Hessami K, Regard V, Bellier O, Vernant P, et al. (2009). Present-day strain distribution across the Minab-Zendan-Palami fault system from dense GPS transects. Geophysical Journal International.179(2):751-62.

-Reasenberg, Paul. (1985). "Second-order moment of central California seismicity, 1969–1982." Journal of Geophysical Research: Solid Earth no. 90 (B7):5479-5495.

- Regard V, Bellier O, Thomas J-C, Bourlès D, Bonnet S, Abbassi MR, et al. (2005). Cumulative right-lateral fault slip rate across the Zagros-Makran transfer zone: role of the Minab-Zendan fault system in accommodating Arabia-Eurasia convergence in southeast Iran. Geophysical Journal International.162(1):177-203.

- Talebian, M., Jackson, J., (2004). A reappraisal of earthquake focal mechanisms and active shortening in the Zagros mountains of Iran. Geophysical Journal International, 156, 506-526.

- Vernant, P., Nilforoushan, F., Hatzfeld, D., Abbassi, M. R., Vigny, C., Masson, F., Tavakoli, F., (2004). Present-day crustal deformation and plate kinematics in the Middle East constrained by GPS measurements in Iran and northern Oman. Geophysical Journal International, 157, 381-398.

- Walker, R. T., Andalibi, M. J., Gheitanchi, M. R., Jackson, J. A., Karegar, S., & Priestley, K., (2005). Seismological and field observations from the 1990 November 6 Furg (Hormozgan) earthquake: a rare case of surface rupture in the Zagros Mountains of Iran. Geophysical Journal International, 163, 567-579.

- Woessner, J., Wiemer, S., (2005). Assessing the quality of earthquake catalogues: Estimating the magnitude of completeness and its uncertainty. Bulletin of the Seismological Society of America, 95, 684-698.